



Discover Generics

Cost-Effective CT & MRI Contrast Agents



WATCH VIDEO

AJNR

Imaging Appearance of *SMARCB1* (INI1)-Deficient Sinonasal Carcinoma: A Newly Described Sinonasal Malignancy

D.R. Shatzkes, L.E. Ginsberg, M. Wong, A.H. Aiken, B.F. Branstetter IV, M.A. Michel and N. Aygun

This information is current as of June 1, 2025.

AJNR Am J Neuroradiol 2016, 37 (10) 1925-1929

doi: <https://doi.org/10.3174/ajnr.A4841>

<http://www.ajnr.org/content/37/10/1925>

Imaging Appearance of *SMARCB1* (INI1)-Deficient Sinonasal Carcinoma: A Newly Described Sinonasal Malignancy

 D.R. Shatzkes,  L.E. Ginsberg,  M. Wong,  A.H. Aiken,  B.F. Branstetter IV,  M.A. Michel, and  N. Aygun



ABSTRACT

SUMMARY: *SMARCB1* (INI1)-deficient sinonasal carcinomas were first described in 2014, and this series of 17 cases represents the first imaging description. This tumor is part of a larger group of *SMARCB1*-deficient neoplasms, characterized by aggressive behavior and a rhabdoid cytopathologic appearance, that affect multiple anatomic sites. Clinical and imaging features overlap considerably with other aggressive sinonasal malignancies such as sinonasal undifferentiated carcinoma, which represents a common initial pathologic diagnosis in this entity. *SMARCB1* (INI1)-deficient sinonasal tumors occurred most frequently in the nasoethmoidal region with invasion of the adjacent orbit and anterior cranial fossa. Avid contrast enhancement, intermediate to low T2 signal, and FDG avidity were frequent imaging features. Approximately half of the lesions demonstrated calcification, some with an unusual “hair on end” appearance, suggesting aggressive periosteal reaction.

Malignancy of the sinonasal cavity is characterized by considerably greater heterogeneity than malignancy of the upper aerodigestive tract, where squamous cell carcinoma predominates. Though squamous cell carcinoma remains the most common sinonasal malignancy (approximately 60% of cases), there is a diverse and growing array of additional histologies, including tumors of epithelial, neuroectodermal, lymphoproliferative, and mesenchymal origins.^{1–4} Though imaging features of the various histologies overlap considerably, some tumors demonstrate characteristic findings that support a particular diagnosis, such as T1 shortening in melanoma or chondroid calcification in chondrosarcoma. Other tumors might demonstrate findings that, though not specific to a single diagnosis, suggest their aggressive nature. Ultimately, tissue sampling is necessary to confirm pathologic diagnosis before treatment planning. Nevertheless, most sinonasal masses present with very nonspecific clinical findings indistinguishable from rhinosinusitis, and the ability of the radiologist to

suggest an underlying malignancy is useful in directing short-term management, including the need for further imaging and tissue sampling.^{3–8}

SMARCB1 (INI1) is a tumor-suppressor gene that has been implicated in a growing number of malignancies involving multiple anatomic sites, including the kidneys, soft tissues, and CNS.^{1,2,9–11} The first reports of *SMARCB1* (INI1)-deficient tumors of the sinonasal cavity appeared in the pathology literature in 2014,^{1,9} followed by an additional small case series in 2015.² To our knowledge, there have been 16 cases reported in the world literature. However, the imaging appearance of *SMARCB1* (INI1)-deficient sinonasal tumors has not yet been described. By analyzing a case series of 17 patients collected from 6 different centers, some of whom were included in the pathologic reports listed above, we aimed to provide a comprehensive description of the appearance of these tumors on CT, MR imaging, and PET/CT studies. We also hoped to increase awareness of this relatively new entity among both radiologists and clinicians to facilitate its diagnosis when encountered in clinical practice.


MATERIALS AND METHODS

This retrospective case series was performed with institutional review board approval and exemption from informed consent following the guidelines of the Health Insurance Portability and Accountability Act. Records of cases presented at our multidisciplinary tumor board since 2014 were reviewed for the pathologic diagnosis of *SMARCB1* (INI1)-deficient sinonasal tumors. In addition, cases were solicited from head and neck radiologists at other medical centers. In all, 17 cases were collected from 6 cen-

Received March 31, 2016; accepted after revision April 22.

From the Department of Radiology (D.R.S., M.W.), Lenox Hill Hospital, Northwell Health, New York, New York; Department of Radiology (L.E.G.), The University of Texas MD Anderson Cancer Center, Houston, Texas; Department of Radiology (A.H.A.), Neuroradiology Division, Emory University Hospital, Atlanta, Georgia; Department of Radiology (B.F.B.), Presbyterian Hospital, Pittsburgh, Pennsylvania; Department of Radiology (M.A.M.), Medical College of Wisconsin, Milwaukee, Wisconsin; and Department of Radiology (N.A.), Johns Hopkins Medicine, Baltimore, Maryland.

Please address correspondence to Deborah R. Shatzkes, MD, Department of Radiology, Lenox Hill Hospital, Northwell Health, 100 E 77th St, New York, NY 10075; e-mail: DShatzkes@northwell.edu

 Indicates article with supplemental on-line table.

<http://dx.doi.org/10.3174/ajnr.A4841>

Patient demographics

Patient	Age (y)	Sex	Original Pathology Diagnosis	Stage Reference ^a	Clinical Status	Published?
1	35	Female	Poorly differentiated carcinoma with squamoid features	T4bN0M0	NED at 10 months	N
2	51	Male	Poorly differentiated carcinoma with glandular differentiation	T4aN0M0	NED at 1 month	N
3	45	Male	Poorly differentiated adenocarcinoma	T4b	NED at 48 months	N
4	50	Female	Poorly differentiated SCC with papillary features	T4aN0M0	NED at 9 months	N
5	72	Male	<i>SMARCB1</i> (INI 1)-deficient sinonasal carcinoma	T4aN0M0	NED at 12 months	N
6	43	Male	Poorly differentiated SCC	T1	NED at 9 months	N
7	59	Male	NA	NA	NED at 12 months	Bishop et al ⁹
8	54	Female	SNUC	T4b	AWD at 6 months	Bishop et al ⁹
9	44	Male	Poorly differentiated basaloid SCC	T4bN0	NED at 18 months	Bishop et al ⁹
10	78	Female	Myoepithelial carcinoma	N0M0	NED at 24 months	Bishop et al ⁹
11	77	Male	Myoepithelial carcinoma	T4bN0M0	DOD at 12 months	Bishop et al ⁹
12	32	Male	SNUC	T4b	AWD at 24 months	Bishop et al ⁹
13	64	Female	SNUC	T4bN0M0	AWD at 13 months	Bell et al ²
14	75	Male	Basaloid SCC	T4bN0M0	NA	Bell et al ²
15	33	Female	High-grade mixed germ cell tumor	T4bN0M0	DOD at 12 months	Bell et al ²
16	51	Female	SNUC	T4N0M0	DOD at 24 months	Bell et al ²
17	62	Male	SNUC	T4bN0M1	NED at 3 months	N

Note:—AWD indicates alive with disease; DOD, dead of disease; N, not previously published; NA, not available; NED, no evidence of disease; SCC, squamous cell carcinoma; SNUC, sinonasal undifferentiated carcinoma.

^aBased on American Joint Commission on Cancer, 7th Edition.

ters, 10 of which were included in prior case series.^{2,9} In most cases, the diagnosis of *SMARCB1* (INI1)-deficient carcinoma represented an amendment of an initial alternate diagnosis. Patient demographics, original pathologic diagnoses, cancer stage, current clinical status, and publication history (where applicable) are summarized in the Table.

All available pretreatment CT, MR imaging, and/or PET/CT studies were reviewed on a PACS or DICOM viewer by a single radiologist with over 20 years of experience in head and neck imaging. MR and PET/CT imaging were available in 14 and 11 patients, respectively. CT images, either as a stand-alone examination or as part of a PET/CT examination, were available in 13 patients. Tumor characteristics compiled were specific location within the sinonasal cavity; the presence of any intracranial, orbital, or perineural extension; and the presence of regional nodal or distant metastases. Imaging parameters included CT attenuation, enhancement, and calcification patterns; MR signal characteristics and enhancement pattern; and the predominant pattern of osseous change. Osseous change was characterized as expansion, erosion, or a combination of both by review of both CT and MR images. PET/CT studies were reviewed for tumor FDG avidity and for the presence of regional nodal or distant metastases. Standard uptake values were unavailable for most of the imaging studies and were not recorded. Similarly, CT and MR imaging technical parameters were not recorded because most imaging was performed at facilities outside of the tertiary centers where the patients were referred for treatment.

RESULTS

Patient Characteristics

Patient characteristics are summarized in the Table. There were 10 men and 7 women, with an average age of 54 years (range, 33–78 years; median 51 years). The initial pathologic diagnoses were sinonasal undifferentiated carcinoma in 5 patients, poorly differentiated carcinoma (squamous, basaloid, adeno, or not otherwise specified) in 6, myoepithelial carcinoma in 2, high-grade

mixed germ cell tumor in 1, and *SMARCB1* (INI1) sinonasal carcinoma in 1. All but 1 patient presented with T4 disease ($n = 15$, T-stage was not available for 2 patients). There were no regional nodal metastases detected in the 12 patients for whom preoperative PET/CT was available. A contralateral mandibular lesion in patient 17 represented the only distant metastasis identified in this subgroup of 12 patients. All patients underwent surgery and variable chemoradiation regimens, and 10 patients were alive without evidence of disease at last available follow-up (average follow-up interval, 14.6 months; range, 1–48 months; median, 11 months). In patient 3, with a follow-up interval of 48 months, the initial pathology was reviewed at the time of suspected recurrence and the diagnosis amended from poorly differentiated adenocarcinoma to *SMARCB1* (INI1)-deficient carcinoma. To date, 4 patients with recurrence are alive and 3 have died.

Tumor Characteristics

Tumor characteristics are summarized in the On-line Table, and representative images are provided in Figs 1 and 2. The most common tumor location was nasoethmoidal ($n = 8$), followed by nasal ($n = 5$) and sphenoethmoidal ($n = 2$), and 1 tumor was centered in the frontoethmoidal region with a large supraorbital component. Another very extensive tumor had components in the nasal cavity and ethmoid, sphenoid, and maxillary sinuses. There was epidural intracranial extension in 8 tumors and intradural extension in 3. Orbital invasion, present in 9 patients, was characterized as extraconal and/or conal in all. In patient 16, a tumor was identified in the cavernous sinus and foramen ovale; this tumor originated in the sphenoethmoidal region, and direct cavernous sinus invasion was suspected. In patient 10, only PET/CT was available and deemed insufficient to accurately assess potential intracranial, intraorbital, or perineural extension. In 2 other patients, imaging was deemed to be of insufficient quality to assess for perineural spread.

Precontrast CT images were available in 8 patients, and the tumor was isoattenuated to skeletal muscle in 6. Contrast en-

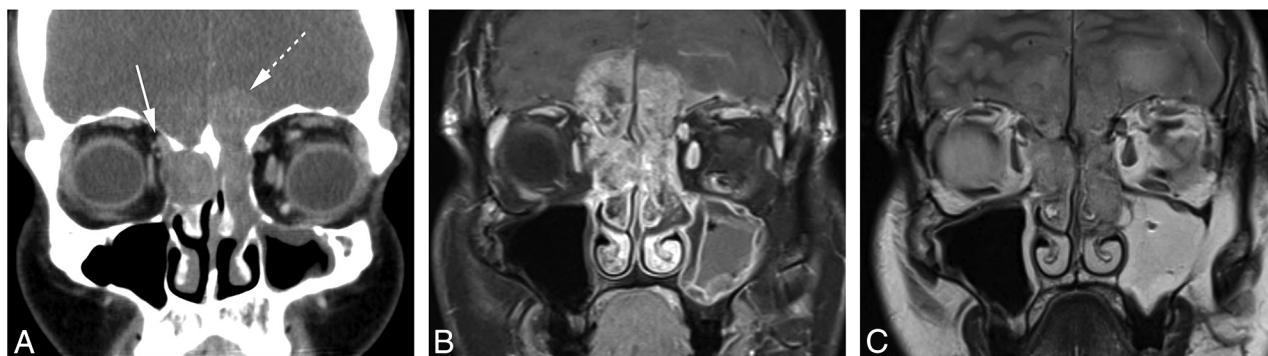


FIG 1. Patient 1. A, Coronal enhanced CT image shows moderately enhancing tumor in the nasoethmoidal region eroding the cribriform plate and ethmoid roof, with intracranial extension more conspicuous on the left (*dashed arrow*). There is also erosion through the right lamina papyracea with contact to the right superior oblique muscle (*solid arrow*). Bone changes in this case were deemed primarily erosive rather than expansile. B, Coronal enhanced and fat-suppressed T1WI shows avid heterogeneous enhancement in the transcranial mass. C, Coronal T2WI shows mild T2 hyperintensity of the transcranial mass compared with the cerebral cortex. Though there is signal abnormality in the left frontal lobe, no intradural disease was identified during surgical resection.



FIG 2. Patient 2. A, Coronal enhanced and fat-suppressed T1WI shows avid heterogeneous enhancement in right nasal cavity mass. There is no intracranial or orbital extension, and this mass was characterized as expansile. B, On this coronal STIR image, the mass is approximately isointense to cerebral cortex and can be distinguished from obstructive secretions in the adjacent ethmoid and maxillary sinuses. C, Coronal fused image from PET/CT examination demonstrates avid uptake in the right nasal cavity mass.

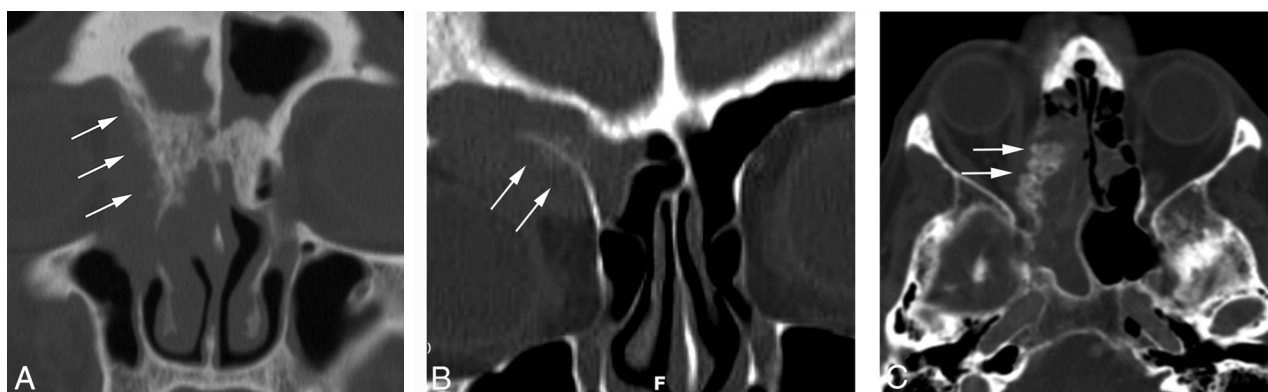


FIG 3. Calcification. A, Patient 9. Coronal CT bone image demonstrates spiculated, “hair on end” calcification along right medial orbital wall, with permeative lytic change in the adjacent bone (*arrows*). B, Patient 13. There is a similar pattern of “hair on end” calcification involving the floor of the right frontal sinus on this coronal CT image (*arrows*). In both patients, the involved bone is demineralized but not destroyed. C, Patient 11. There is a more solid, floccular pattern of calcification along the right medial orbital wall on this axial CT image (*arrows*).

hancement of the tumor was identified in all 7 patients for whom both pre- and postcontrast CT images were available. This was graded as moderate in 6 patients and avid in 1 and further characterized as heterogeneous in 6. Calcification was present in 6 of the 13 patients for whom CT imaging was available. In 3 pa-

tients, there was a spiculated “hair on end” pattern of calcification along the interface, with adjacent bone suggesting aggressive periosteal reaction (Fig 3). In patient 11, floccular calcification present along the margin of the tumor with the medial orbital wall was deemed to potentially represent a more solid pattern of periosteal

reaction. In 2 patients, stippled and curvilinear calcifications were present within the tumor, thought to likely represent retained bone fragments within a background of bone destruction. The impact on adjacent bony structures was assessed on both CT and MR imaging. Bone changes were classified as predominantly erosive in 9 patients, expansile in 5, and a combination of expansile and erosive in 3.

The tumor was isointense to cortex in 11 of the 14 patients for whom precontrast T1WI was available. In the remaining 3 patients, the tumor was graded as mildly hypointense. The tumor was variably mildly hypointense ($n = 4$), isointense ($n = 4$), moderately hyperintense ($n = 3$), and mildly hyperintense ($n = 3$) to cortex on T2WI. Enhancement was graded as avid in 11 of the 14 patients for whom postcontrast MR imaging was available, with the remaining tumors demonstrating moderate enhancement. Enhancement was additionally characterized as heterogeneous ($n = 7$) and homogeneous ($n = 7$). DWI was available for 9 patients. Most lesions ($n = 7$) showed moderate diffusion restriction.

FDG uptake was demonstrated in all 12 patients who underwent PET/CT scanning. Radiotracer uptake was graded as avid in 9 patients and moderate in 3.

DISCUSSION

SMARCB1 is a tumor-suppressor gene located on chromosome 22q11.2.^{1,2,9,10} Deficiency of *SMARCB1* (INI1) was first implicated in malignant rhabdoid tumors of infancy, followed by rhabdoid tumor of the CNS, kidney, and soft tissue.^{1,2,9,10} This list has since grown to include a diverse group of neoplasms in multiple anatomic sites, all of which are characterized by a rhabdoid appearance on cytopathologic examination and generally aggressive behavior.^{1,2,9,10} The first descriptions of *SMARCB1* (INI1)-deficient neoplasms of the sinonasal tract were published simultaneously in the pathology literature by 2 separate groups in September 2014.^{1,9} A third case series, completing a total of 16 reported cases, was published in September 2015.² Our series, with an additional 7 cases, represents the fourth report and the first detailed imaging description of this entity.

It is difficult to estimate the prevalence of this disease because most cases were initially diagnosed as other high-grade malignant tumors, most commonly sinonasal undifferentiated carcinoma and other poorly differentiated carcinomas often qualified as having rhabdoid or basaloid features. In their review of their own cases and those previously reported, Bell et al² found that *SMARCB1* (INI1)-deficient sinonasal carcinomas represented 3.3% of a combined series of 484 sinonasal primary tumors. However, Bishop et al⁹ noted that *SMARCB1* (INI1)-deficient sinonasal carcinomas represented 14% of previously diagnosed sinonasal undifferentiated carcinomas.⁹ More accurate estimates will likely be available once the diagnosis is more widely known in the head and neck oncologic community.

There are few sinonasal tumors with highly characteristic or pathognomonic imaging or clinical features, and this tumor is no exception. With regard to patient demographics, the wide age range and median age of 51 years overlap with virtually all sinonasal malignancies except those found in pediatric age groups, such as juvenile nasopharyngeal angiofibroma and rhabdomyo-

sarcoma. A clear predilection for late-stage presentation was identified in our series, with only 1 patient staged below T4. However, this is the case in most aggressive sinonasal malignancies.^{6,8,12,13} We found a predilection for central structures, with 13 of 17 tumors described as nasal or nasoethmoidal in origin, with frequent invasion into the adjacent orbital and intracranial compartments. Other sinonasal malignancies such as sinonasal undifferentiated carcinoma, esthesioneuroblastoma, lymphoma, and melanoma arise most frequently in the superior nasal cavity with similar patterns of invasion. The tendency toward avid enhancement, intermediate T2 signal intensity, moderate diffusion restriction, and FDG avidity demonstrated in our series is characteristic for sinonasal undifferentiated carcinoma and squamous cell carcinoma, which, though occurring most commonly in the paranasal sinuses (75%), must still be considered when nasal cavity masses are identified because of the high relative prevalence of this diagnosis.^{1-4,7,12} CT imaging demonstrated associated calcification in close to half of the tumors (6 of 13), though no tumor calcification was reported on histopathologic analysis. In considering this discrepancy, we felt that calcification might reflect retained bone fragments in 2 patients and an aggressive periosteal reaction in 4. Nevertheless, our observed frequency of calcification on CT exceeds that reported in the literature, and the perpendicular “hair on end” appearance suggesting aggressive periosteal reaction is a particularly unusual feature.^{5,7,12,14} A more accurate estimation of the incidence of this and other imaging features, and of their potential utility as indicators of this disease, will require a larger sample size.

Limitations

In addition to the small sample size, other substantial limitations are related to the pooling of data from multiple centers. Much of the imaging reviewed was performed outside of these tertiary referral centers, and both imaging protocols and quality varied widely. Technical specifications of scanners and specifics of pulse sequence parameters were generally unavailable and were not compiled. There were similar limitations on the availability of clinical information, and length of follow-up was necessarily limited because of the short interval after initial description of the entity. There are few prospectively acquired data regarding imaging appearance of sinonasal malignancies, and available information is largely limited to relatively small case series such as ours. Therefore, comparisons with other sinonasal malignancies are fraught with similar limitations of small sample size and heterogeneous data.

CONCLUSIONS

The recently described entity of *SMARCB1* (INI1)-deficient sinonasal carcinoma should be included in the differential diagnosis of a central sinonasal mass demonstrating aggressive imaging features, particularly when there is associated calcification. Overlap in clinical and imaging features of *SMARCB1* (INI1)-deficient carcinoma with other sinonasal malignancies, such as sinonasal undifferentiated carcinoma, underscores the challenges currently faced in diagnosis of these entities. The presence of rhabdoid features on cytopathologic examination will help alert pathologists and clinicians to the possibility of this diagnosis so confirmation

can be achieved using appropriate testing. As the diagnosis becomes more widely known, we anticipate the opportunity for larger series and more accurate assessment of clinical and imaging features of this disease.

ACKNOWLEDGMENTS

The authors gratefully acknowledge contribution of case material from Drs. Justin A. Bishop and John M. DelGaudio.

Disclosures: Michelle A. Michel—UNRELATED: Payment for Lectures (including service on speakers bureaus); iiCME, Comments: lectured at a continuing medical education course in January 2016 and received honoraria; Royalties: Elsevier, Comments: received a royalty check for prior contributions to *Diagnostic Imaging* textbooks; Stock/Stock Options: Fidelity, Transamerica, Comments: personal investments only.

REFERENCES

1. Agaimy A, Koch M, Lell M, et al. **SMARCB1 (INI1)-deficient sinonasal basaloid carcinoma: a novel member of the expanding family of SMARCB1-deficient neoplasms.** *Am J Surg Pathol* 2014;38:1274–81 CrossRef Medline
2. Bell D, Hanna EY, Agaimy, et al. **Reappraisal of sinonasal undifferentiated carcinoma: SMARCB1 (INI1)-deficient sinonasal carcinoma: a single-institution experience.** *Virchows Arch* 2015; 467:649–56 CrossRef Medline
3. Eggesbø HB. **Imaging of sinonasal tumours.** *Cancer Imaging* 2012; 12:136–52 CrossRef
4. Sen S, Chandra A, Mukhopadhyay S, et al. **Sinonasal tumors: computed tomography and MR imaging features.** *Neuroimaging Clin N Am* 2015;25:595–618 CrossRef Medline
5. Loevner LA, Sonners AI. **Imaging of neoplasms of the paranasal sinuses.** *Neuroimaging Clin N Am* 2004;14:625–46 CrossRef Medline
6. Lund VJ, Stammberger H, Nicolai P, et al. **European position paper on endoscopic management of tumours of the nose, paranasal sinuses and skull base.** *Rhinol Suppl* 2010;22:1–143 Medline
7. Phillips CD, Futterer SF, Lipper MH, et al. **Sinonasal undifferentiated carcinoma: CT and MR imaging of an uncommon neoplasm of the nasal cavity.** *Radiology* 1997;202:477–80 CrossRef Medline
8. Sen S, Chandra A, Mukhopadhyay S, et al. **Imaging approach to sinonasal neoplasms.** *Neuroimaging Clin N Am* 2015;25:577–93 CrossRef Medline
9. Bishop JA, Antonescu CR, Westra WH. **SMARCB1 (INI-1)-deficient carcinomas of the sinonasal tract.** *Am J Surg Pathol* 2014;38:1282–89 CrossRef Medline
10. Bishop JA. **Newly described tumor entities in sinonasal tract pathology.** *Head Neck Pathol* 2016;10:23–31 CrossRef Medline
11. Kalimuthu SN, Chetty R. **Gene of the month: SMARCB1.** *J Clin Pathol* 2016;69:484–89 CrossRef Medline
12. Sivalingam J, Sarawagi R, Raghuvanshi S, et al. **Sinonasal neoplasia: clinicopathological profile and importance of computed tomography.** *J Clin Diagn Res* 2015;9:TC01–4 CrossRef Medline
13. Xu CC, Dziegielewska PT, McGaw WT, et al. **Sinonasal undifferentiated carcinoma (SNUC): the Alberta experience and literature review.** *J Otolaryngol Head Neck Surg* 2013;42:2 CrossRef Medline
14. Rana RS, Wu JS, Eisenberg RL. **Periosteal reaction.** *AJR Am J Roentgenol* 2009;193:W259–72 CrossRef Medline